

Geophysical Research Letters[®]

RESEARCH LETTER

10.1029/2022GL100958

Key Points:

- Intense 2021 North American heat wave is associated with extremely amplified upper-level ridge
- Magnitude of record-high temperatures was not predicted beyond 7 days
- Chain of synoptic-scale precipitation events constitutes predictability barrier

Supporting Information:

Supporting Information may be found in the online version of this article.

Correspondence to:

A. Oertel,
annika.oertel@kit.edu

Citation:

Oertel, A., Pickl, M., Quinting, J. F., Hauser, S., Wandel, J., Magnusson, L., et al. (2023). Everything hits at once: How remote rainfall matters for the prediction of the 2021 North American heat wave. *Geophysical Research Letters*, 50, e2022GL100958. <https://doi.org/10.1029/2022GL100958>

Received 26 AUG 2022

Accepted 21 JAN 2023

© 2023. The Authors.

This is an open access article under the terms of the [Creative Commons Attribution-NonCommercial License](https://creativecommons.org/licenses/by/4.0/), which permits use, distribution and reproduction in any medium, provided the original work is properly cited and is not used for commercial purposes.

Everything Hits at Once: How Remote Rainfall Matters for the Prediction of the 2021 North American Heat Wave

A. Oertel¹ , M. Pickl¹ , J. F. Quinting¹ , S. Hauser¹ , J. Wandel¹ , L. Magnusson², M. Balmaseda² , F. Vitart² , and C. M. Grams¹ 

¹Institute of Meteorology and Climate Research (IMK-TRO), Karlsruhe Institute of Technology (KIT), Karlsruhe, Germany,

²European Centre for Medium-Range Weather Forecasts (ECMWF), Reading, UK

Abstract In June 2021, Western North America experienced an intense heat wave with unprecedented temperatures and far-reaching socio-economic consequences. Anomalous rainfall in the West Pacific triggers a cascade of weather events across the Pacific, which build up a high-amplitude ridge over Canada and ultimately lead to the heat wave. We show that the response of the jet stream to diabatically enhanced ascending motion in extratropical cyclones represents a predictability barrier with regard to the heat wave magnitude. Therefore, probabilistic weather forecasts are only able to predict the extremity of the heat wave once the complex cascade of weather events is captured. Our results highlight the key role of the sequence of individual weather events in limiting the predictability of this extreme event. We therefore conclude that it is not sufficient to consider such rare events in isolation but it is essential to account for the whole cascade over different spatiotemporal scales.

Plain Language Summary In June 2021, Western North America experienced an intense heat wave with unprecedented temperatures and far-reaching socio-economic consequences. We show that the forecast of the extreme temperature anomalies was limited due to a complex sequence of weather events across the Pacific. Thus, state-of-the-art weather forecasts were only able to predict the magnitude of the heat wave once the cascade of weather events was captured in the forecast.

1. Introduction

The heat wave during the end of June 2021 in Western North America was unprecedented. In Lytton, British Columbia, Canada's previous all-time maximum temperature record dating back to 1937 was exceeded on 29 June by 5 K (Abraham, 2021; Philip et al., 2021). Although heat waves are expected to become hotter in a changing climate (Seneviratne et al., 2021) and the probability of record-breaking extremes with temperatures well above previous records will increase (Fischer et al., 2021), early attribution studies suggest that even under consideration of the current state of climate change, the temperatures of this event were extraordinarily unusual (Philip et al., 2021): the 2-m temperature anomaly with respect to the June to July climatological mean from 1979 to 2019 reached up to 20 K (Figure 1a). It is well-known that such extratropical heat waves are typically linked to persistent, quasi-stationary, strongly amplified, upper-level ridges that are embedded in extratropical Rossby waves (Coumou et al., 2018; Hoskins & Woollings, 2015; Kornhuber et al., 2020; Petoukhov et al., 2016; Screen & Simmonds, 2014; Spensberger et al., 2020; Teng et al., 2013) and cause anomalous temperatures through air-mass advection, large-scale subsidence, and clear-sky radiation (Bieli et al., 2015; Pfahl & Wernli, 2012; Quinting & Reeder, 2017; Zschenderlein et al., 2019). The heat wave in Western North America also occurred underneath a high-amplitude quasi-stationary upper-tropospheric ridge (Figure 1a) which was colloquially coined as “heat dome” (Capuccini & Samenow, 2021; Philip et al., 2021). The upper-tropospheric ridge was characterized by a quasi-stationary negative potential vorticity (PV; Hoskins et al., 1985) anomaly that extended from the northwestern U.S. into the Canadian Northwest territories (Figure 1a and Figure S4 in Supporting Information S1). Large-scale subsidence underneath this high-amplitude ridge together with quasi-local diabatic heating contributed to the unusual near-surface temperatures (Qian et al., 2022). Moreover, warm air advection and enhanced lower-tropospheric to midtropospheric moisture in the region of an atmospheric river trapped the long-wave radiation and thus amplified the temperature anomaly further (Mo et al., 2022). At subseasonal time scales with lead times of >2–3 weeks, various subseasonal-to-seasonal prediction models already captured above-normal temperatures in Western North American (Emerton et al., 2022; Lin et al., 2022). Yet, the extreme magnitude of the heat wave was not captured by state-of-the-art numerical weather prediction models at forecast lead times beyond ~7 days (Figure 1b; see also Lin et al., 2022). Only at lead times of <7 days, the extreme and

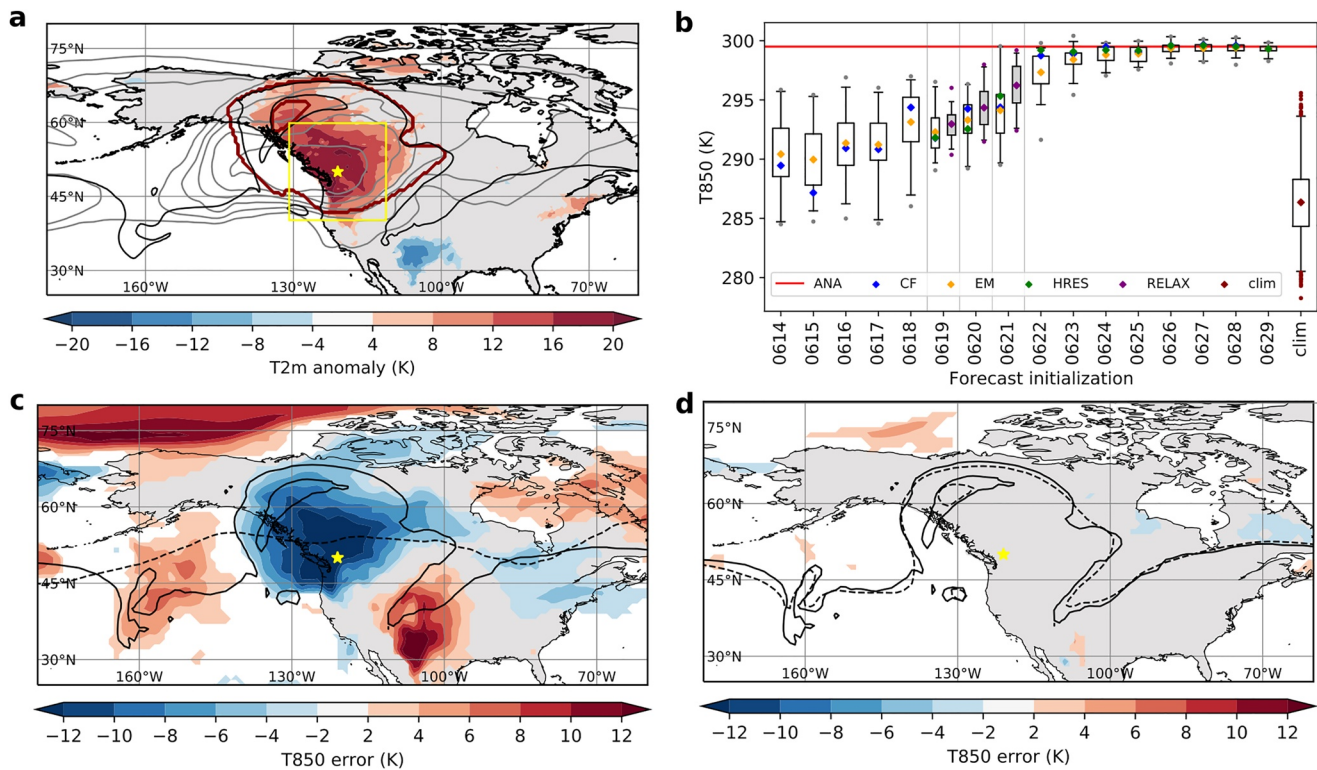


Figure 1. (a) ERA5 2-m temperature anomaly on 29 June 2021 00 UTC with respect to the June/July ERA5 climatology from 1979 to 2019 (shading in K). Shown are the 2 PVU contour on the 335 K isentrope (black), the upper-level negative potential vorticity (PV)-anomaly object (red; Section 2), frequencies of such negative PV anomalies between 13 June and 04 July (gray contour intervals are 2%, 10%, 20%, 30%, 40%, and 50%), and the position of Lytton, BC (yellow star). (b) Distributions of ensemble forecasts of 850-hPa temperature valid on 29 June 2021 00 UTC averaged over the yellow $20^{\circ} \times 20^{\circ}$ box around Lytton, reflecting the hot air mass, initialized daily at 00 UTC between 14 and 29 June 2021. Colored diamonds represent the control forecast (blue), the ensemble mean (orange) and the high-resolution forecast (green), the box (whiskers) marks the 25–75 interquartile (1–99 interquartile) range, and the gray dots represent the maximum and minimum values. Gray boxes and purple diamonds represent the ensemble distribution and mean, respectively, of the relaxation experiments initialized on 19–21 June (see Section 3.3). The red line represents the analyzed (ERA5) 850-hPa temperature. The box (whiskers) located at the label “clim” shows the 25–75 interquartile (1–99 interquartile) range of the 30-day ERA5 climatology from 15 June to 14 July between 1979 and 2019, and the dots show values beyond the 1st and 99th percentiles. (c) Composite-mean 850-hPa temperature errors (shading in K) and 2 PVU contour on 335 K (dashed line) of forecasts in the “bad” category ($n = 230$), and analyzed 2 PVU contour on 335 K (solid line) valid on 29 June 00 UTC (see Section 2 for a details on the forecast classification). (d) As c, but for the “good” forecasts ($n = 230$).

unprecedented temperatures in Western North America were predicted by the ensemble forecasting system of the European Centre for Medium-Range Weather Forecasts (ECMWF; Figure 1b; see Emerton et al. (2022) for ECMWF forecasts of 2-m temperature). The relatively short lead time due to insufficient medium-range forecasts may have hampered possible disaster mitigation efforts, which may require more time than the predictability horizon of the event (White et al., 2017). On 22 June, 7 days prior to the peak of the heat wave, the forecasts of temperature near the surface (not shown) and at 850 hPa ($T@850$ hPa), which is in ~ 1.5 -km height above sea level and characterizes the regional air mass, abruptly improved (Figure 1b). Subsequent forecasts captured the record-breaking heat anomaly and the corresponding large-scale flow pattern, indicating the existence of a predictability barrier (González-Alemán et al., 2022; Sánchez et al., 2020) on the synoptic time scale, which hinders successful predictions of the intense heat on the medium-range time scale extending to up to 15 days lead time. Here, we apply an atmospheric dynamics perspective focusing on the critical role of the chain of synoptic events leading to the strong amplification of the upper-level flow and limiting the medium-range predictability of this extreme event. Specifically, we focus on the influence of episodes of strongly ascending airstreams, henceforth referred to as warm conveyor belts (WCBs), on the North Pacific jet stream and subsequent ridge amplification.

2. Methodology

Throughout this study, we use a number of different methodological approaches, including the Lagrangian and Eulerian perspectives of diabatically enhanced ascending airstreams, so-called WCBs (e.g., Grams & Archambault, 2016; Grams et al., 2018; Madonna et al., 2014; Wernli & Davies, 1997).

We employ a Lagrangian perspective to highlight the remote influence and the role of diabatically enhanced ascending airstreams for the formation of the upper-level ridge. Based on 3-hourly wind fields from the ERA5 reanalysis (Hersbach et al., 2020), 10-day backward trajectories are started on 29 June 00 UTC within the upper-level ridge between 500 and 150 hPa using LAGRANTO (Sprenger & Wernli, 2015; Wernli & Davies, 1997). Specifically, trajectories are initialized within the negative PV-anomaly object identified as a vertically averaged PV anomaly between 500 and 150 hPa with a deviation of at least -0.69 PVU (potential vorticity units) from the 30-day running mean climatology for 1979–2019 (Hauser et al., 2022). Only such trajectories that originate from below 800 hPa, i.e., substantially ascend prior to their arrival in the ridge, are considered (Figure 2a). Subsequently, the remaining trajectories are classified by the location where (West or East Pacific) and when their main ascent occurs (Figure 2b).

To identify processes that influenced the predictability of the heat wave magnitude and that led to the formation of the upper-level ridge over North America, we make use of operational ECMWF ensemble forecasts. The considered forecasts are initialized daily at 00 UTC between 14 and 29 June 2021 and have been retrieved on a $1^\circ \times 1^\circ$ grid. The ensemble comprises 50 perturbed members plus one control forecast. Based on the representation of the upper-level ridge over North America, each of the 765 individual medium-range ensemble forecasts initialized between 14 and 28 June at 00 UTC is classified into a group of “good” or “bad” forecasts (Figure S1 in Supporting Information S1). This classification is based on the percentile rank of the domain-average root-mean squared error (RMSE) of potential temperature at the 2 PVU isosurface in the upper-level ridge (145° – 95° W, 30° – 75° N) valid on 29 June 00 UTC, verified against ECMWF's operational high-resolution analysis. Forecasts with the 30% lowest and highest RMSE are grouped into the “good” and “bad” categories, respectively, with overall 230 individual forecasts in each group. Within these subgroups, imprints of WCBs are detected by using a novel technique based on convolutional neural networks (ELIAS2.0; Quinting & Grams, 2022; Quinting et al., 2022; Supplementary Methods in Supporting Information S1).

3. Results

3.1. Heat Wave Unambiguously Linked to Upper-Level Ridge

To emphasize the dominant role of synoptic events in limiting the predictability of the heat wave magnitude, we analyze the evolution of the upper-level flow in the “good” forecasts and compare them to the “bad” forecasts, which have the largest discrepancy in the upper-level flow field (Section 2). “Good” forecasts are solely initialized after 22 June while all “bad” forecasts are initialized before 23 June (see Figure S1 in Supporting Information S1), emphasizing the presence of the medium-range predictability barrier on 22 June, i.e., after the abrupt improvement in the T@850 hPa ensemble forecast (Figure 1b). The selected “good” forecasts that adequately represent the position and amplitude of the upper-level ridge also correctly represent the temperature anomaly at 850 hPa (Figure 1d). In contrast, the “bad” forecasts with the largest error in the tropopause height also strongly underestimate the temperature where the heat wave occurred (Figure 1c). For example, near Lytton, T@850 hPa was underestimated on average by almost 14 K in the “bad” forecasts. The “bad” forecasts are characterized by a too zonal flow across the Pacific and a strong underestimation of the extent of the upper-level ridge (Figure 1c), and thus, of the heat dome. We conclude that the large-scale, far poleward extending upper-level ridge with anomalously high tropopause heights (Figure S2 in Supporting Information S1) is a prerequisite for the recorded temperature extremes, and that correct predictions of the heat wave magnitude are unambiguously linked to the correct representation of the ridge amplitude.

3.2. High-Amplitude Ridge Influenced by Complex Chain of Synoptic Events

The upper-level ridge was continuously fed by air masses originating to a substantial fraction from the lower troposphere over the North Pacific during the 10 days prior to the heat wave (Figure 2a). Diabatically enhanced cross-isentropic ascent and subsequent outflow near the tropopause further downstream and poleward is

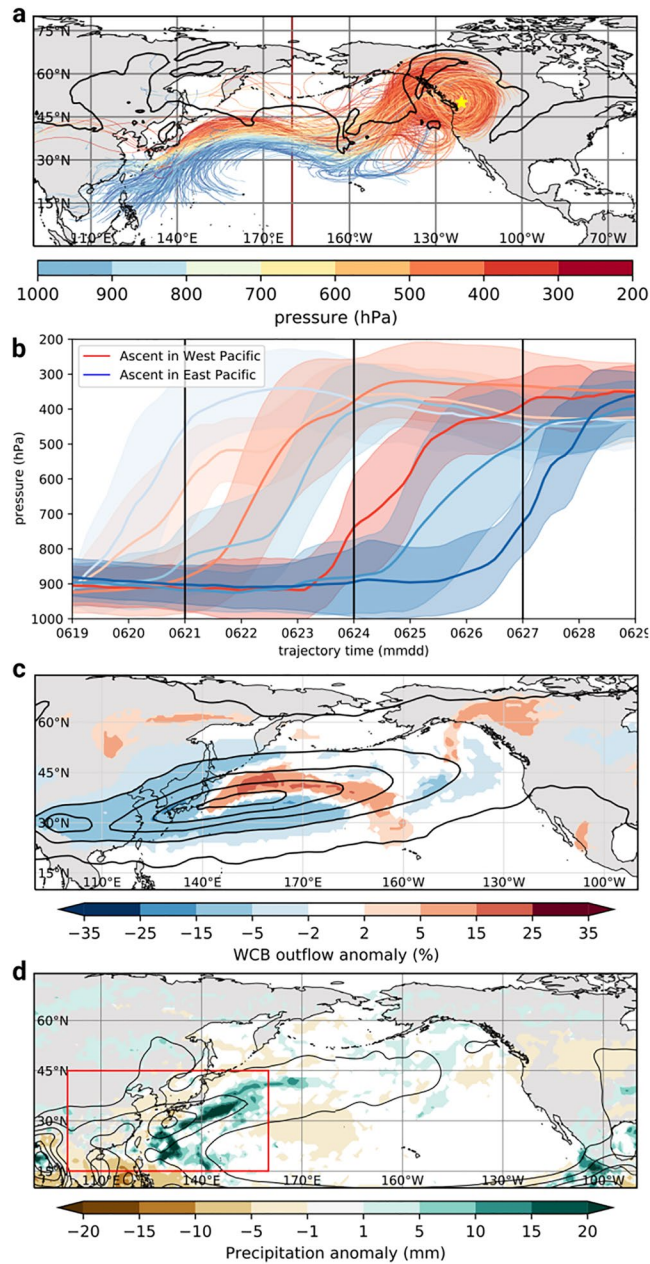


Figure 2. (a) Ten-day backward trajectories initialized within the upper-level ridge over North America on 29 June 00 UTC (see Figure 1a) which are located below 800 hPa 10 days earlier. In total, 20% of all trajectories ($n = 1,249$) ascend from the lower troposphere into the upper-level ridge. The red line at 180°E marks the separation of the West and East Pacific. (b) Mean (colored lines) and standard deviation (shading) of the evolution of pressure along trajectories shown for trajectory clusters separated by their ascent position (red for West Pacific, blue for East Pacific) and the time interval when the ascent occurs. About 51% of the trajectories ascend in the West Pacific, 46% in the East Pacific, and 3% of the trajectories are not categorized. (c) 15–29 June anomalies (shading) and 40-year June ERA5 climatologies (contours) of warm conveyor belt (WCB) outflow (contour intervals at 0.5%, 5%, 10%, 15%, and 20%) based on the convolutional neural networks model ELIAS2.0. (d) 15–29 June anomalies (shading) and 22-year (2000–2021) climatology of daily GPM IMERG precipitation (Huffman et al., 2019) for June (contour intervals at 3, 6, 9, 12, 15, 18, and 21 mm/day). The red box depicts the relaxation domain for the tailored relaxation experiments (see Supplementary Methods in Supporting Information S1).

an effective physical mechanism for initiating, amplifying, and maintaining an upper-tropospheric ridge (Ahmadi-Givi et al., 2004; Grams & Archambault, 2016; Haynes & McIntyre, 1987; Pfahl et al., 2015; Steinfeld & Pfahl, 2019). Latent heat release in an ascending, precipitating airstream, such as the WCB, triggers a net transport of low-PV air into the upper troposphere (Grams et al., 2013), where climatologically high stratospheric

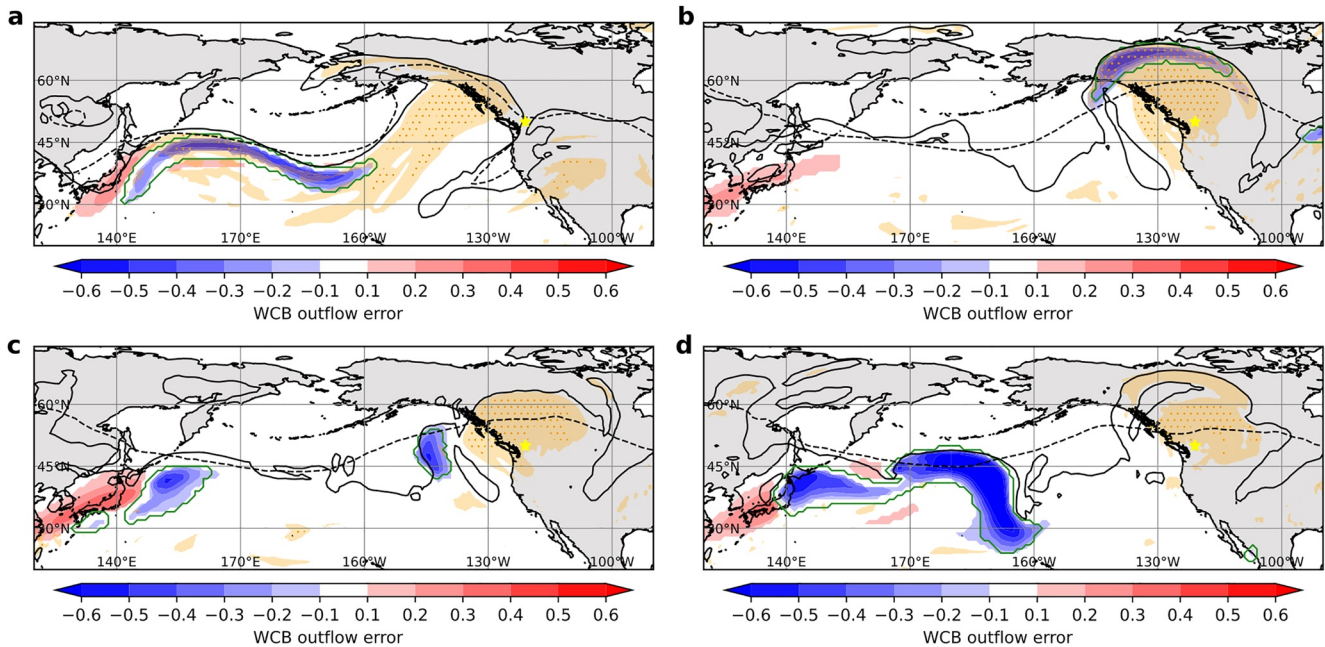


Figure 3. Composite-mean warm conveyor belt (WCB) outflow frequency errors (shading) and 2 PVU line on the 335 K isentrope (dashed line) of “bad” forecasts. The area enclosed by the green line shows WCB outflow in the analysis and the solid black line indicates the analyzed position of the 335 K 2 PVU line. The orange shading (hatching) highlights regions where the tropopause height (i.e., potential temperature on 2 PVU) exceeds the 95th (99th) percentile of the ERA5 data set (see Supplementary Methods in Supporting Information S1). Panel a is valid on 24 June, b on 27 June, c on 28 June, and d on 29 June.

PV values prevail (Madonna et al., 2014). This results in a pronounced anticyclonic PV anomaly downstream of the ascent region. The poleward and upward injection of low-PV air, furthermore lifts the tropopause and strengthens the tropopause PV-gradient accelerating the jet stream. Thus, cross-isentropic air mass transport initiated through latent heat release in a precipitating airstream is an effective way to initiate ridge-building, the amplification and downstream development of Rossby waves along the jet stream, and the evolution of a blocking anticyclone (Grams & Archambault, 2016; Pfahl et al., 2015). Indeed, this physical mechanism was at play during the 2021 North American heat wave as discussed in the following.

The investigation of WCB activity around the 2021 North American heat wave based on ERA5 reanalysis 10-day backward trajectories from the upper-level ridge reveals that 20% of the air mass in the ridge originate from below 800 hPa and are heated diabatically. Within 3 days prior to their arrival in the upper-level PV anomaly 18% of all trajectories are heated by >2 K, while this fraction increases to 48% if the time span is extended to 7 days (cf. Pfahl et al., 2015; Steinfeld & Pfahl, 2019). We furthermore identified individual ascent episodes across the North Pacific. WCB ascent took place predominantly in the West and East Pacific on 21–24 June, and later only in the East Pacific on 25–28 June (Figure 2b). The role of WCB ascent in the East Pacific on 22/23 June for initial ridge amplification was highlighted by Neal et al. (2022). The second ascent period over the East Pacific is linked to the occurrence of atmospheric rivers (cf. Figure 2 in Mo et al. (2022)) which most likely provided moisture to the ascending WCBs. We also identify an early WCB ascent episode prior to 21 June where WCB trajectories ascending in the West Pacific reach the upper troposphere and contribute to the ridge's air mass.

In the following, we discuss the role of ascending air masses in both regions for the amplification and maintenance of the ridge over Western North America. This will also highlight the challenge for numerical weather prediction models to correctly predict the sequence of many individual synoptic events which eventually formed the high-amplitude upper-level ridge facilitating extreme temperatures.

During the 3 days prior to the peak of the heat wave, the ascending air masses over the East Pacific (Figures 3b and 3c, green contours based on analysis data) are directly fed into the upper-level ridge (Figures 3b and 3c, black contour). The most rapidly ascending airstreams reach the ridge on its upstream and poleward flank. A North-South cross-section through the ridge and associated WCB outflow illustrates this diabatically enhanced

ridge-building (Figure S3 in Supporting Information S1): In the “good” forecasts, which also correctly represent WCB activity (see Section 3.3), the ridge is reflected in a very high dynamical tropopause (2-PVU isoline) above 200 hPa between 45°N and 60°N (Figure S3a in Supporting Information S1). At the same time, the cross-isentropic air mass injection is reflected in the large vertical separation of the 330 K isentrope at 500 hPa and the 345 K isentrope at 200 hPa in a region of a strong negative PV anomaly. In the “bad” forecasts, these features are absent and the two isentropes are located at pressure heights of 400 and 250 hPa, respectively (Figure S3b in Supporting Information S1). Thus, the cross-isentropic air mass transport supported by latent heat release within WCBs importantly contributed to the amplitude of the upper-level ridge. The collocation of WCB outflow and anomalously high tropopause heights exceeding the 95th percentile of the climatological height (Figures 3b and 3c, orange shading and stippling) gives further evidence that also for this event the WCB outflow maintains the quasi-stationary ridge, reamplifies the pre-existing PV anomaly and finally leads to a poleward extension of the ridge (Figures 3a–3c and S2d–S2f in Supporting Information S1). The East Pacific WCB events are triggered through downstream baroclinic development across the North Pacific a few days earlier (Figures 3a and 3b). An initially small amplification of the upper-level Rossby wave in the West Pacific (Figure 3a) and subsequent development of a ridge-trough pattern in the Central Pacific enables cyclogenesis and WCB ascent ahead of the formed trough. The amplification of the Rossby wave in the West Pacific is associated with the ascending air masses between 21 and 24 June over the West and Central Pacific. On 24 June, the outflow of WCBs over the West Pacific is juxtaposed with the dynamical tropopause (Figure 3a). Its anomalous height exceeding the 95th percentile of the climatological value in this region indicates the important contribution of the ascending airstreams to the lifting of the tropopause. The exceptionally high tropopause air mass is transported downstream, as indicated by the trajectories (Figures 2a and 2b), and represents an important preconditioning for extreme tropopause heights in the ridge over Western North America.

The significant contribution of diabatic processes and WCB outflow to the anomalous tropopause height is finally confirmed from a climatological perspective (see Supplementary Methods in Supporting Information S1): during 10 days prior to the peak of the heat wave, the WCB activity across the North Pacific was unusually high, particularly for summer conditions (Figure 2c). In the East Pacific, the WCB outflow frequency locally exceeds the June climatological mean value by a factor of 10 (Figure 2c). In the West Pacific, the quasi-stationary Meiyu-Baiu-Front leads to a local maximum of climatological WCB activity (Ding & Chan, 2005; Madonna et al., 2014; Ninomiya & Shibagaki, 2007) (black contours in Figure 2c). Prior to the heat wave, however, the WCB activity is shifted northeast, resulting in anomalously high WCB activity in the Western and Central Pacific which exceeds the climatological mean value by a factor of 2 (Figure 2c). The anomalous WCB activity in the West Pacific coincides with a strong precipitation anomaly: satellite observations (see Supplementary Methods in Supporting Information S1) emphasize the above-normal rainfall that occurred in the second half of June near the Meiyu-Baiu-Front (Figure 2d). In this region, between 19 and 23 June, substantial precipitation is associated with WCB ascent, whose outflow plays an important role in preamplification of the upper-level jet (Figure 3a). All this corroborates the importance of diabatic processes for the WCB outflow and the lifting of the tropopause as a preconditioning of the highly amplified Rossby wave pattern across the North Pacific.

3.3. Synoptic-Scale Processes Limit Predictability

The above analysis suggests that the complex interplay of synoptic events over the West and East Pacific contributed significantly to the upper-level ridge over North America. In the following, we will highlight the importance of this interplay for the correct prediction of the heat wave by evaluating ECMWF's ensemble forecasts. The analysis of WCB activity in all individual forecasts (see Section 2) shows that forecasts which are characterized by large errors in both the upper-level flow and $T@850$ hPa (i.e., the “bad” forecasts) consistently underestimate WCB ascent and upper-level outflow across the West and East Pacific prior to the event (Figure 3). Concerning the WCB activity over the East Pacific, the “bad” forecasts systematically underestimate the WCB activity 3 days prior to the event (Figures 3b and 3c), which results in a misrepresentation of the final ridge position and amplitude (Figure 3d). This underestimation of WCB activity over the East Pacific and the subsequent misrepresentation of the upper-level ridge is linked to erroneous WCB outflow in the West Pacific on 24 June (Figure 3a). This diabatic outflow in the West Pacific amplifies the upper-level Rossby wave pattern and subsequently enables WCB ascent ahead of the developing trough downstream (Figure 3b). The “bad” forecasts position WCB outflow and the associated ridge too far to the west (Figure 3a), and thus miss the correct downstream flow evolution. To summarize, the misrepresentation of WCB outflow in the West Pacific (Figure 3a) and its interaction with

the upper-level jet leads to an underestimation of WCB activity in the East Pacific (Figures 3b and 3c), finally resulting in an erroneous position and amplitude of the upper-level ridge (Figure 3d). The considerable underestimation of the temperature under a too weakly amplified ridge by the “bad” forecasts highlights the relevance of this specific chain of synoptic events for the occurrence and prediction of such rare temperature extremes.

To address the role of West Pacific precipitation for the predictability barrier for the Western North American heat wave, tailored relaxation experiments were performed (Magnusson, 2017). For that purpose, ensemble reforecasts were initialized on 19–21 June and were drawn toward the truth in the region surrounding the West Pacific precipitation anomaly (see Supplementary Methods in Supporting Information S1). The improved representation of the atmospheric state in the West Pacific during the intense precipitation events (cf. Figure 2d) improves the forecast of the heat wave: the upper-level flow across the Pacific is represented more accurately, and in particular, the development of the Central Pacific trough on 27 and 28 June improves (Figure S5 in Supporting Information S1). The representation of the final ridge position in the relaxation experiments on 29 June is improved, in particular its westward extension and the position of the upstream trough. Nevertheless, the poleward extent is still underestimated (Figure S5 in Supporting Information S1). Accordingly, the temperature is still too low in the relaxation experiments (gray boxes and purple diamonds in Figure 1b), although the ensemble mean is increased compared to the operational forecasts (Figure S5 in Supporting Information S1) and the ensemble distribution is shifted closer to the magnitude of the heat wave (Figure 1b). Thus, the correct representation of the interaction of precipitation with the atmospheric flow in the West Pacific leads to improved, yet imperfect forecasts. For comparison, the same nudging experiments were performed with relaxation in a box shifted further upstream. These experiments, however, did not improve the forecast of the heat wave (Figure S6 in Supporting Information S1). We conclude that precipitation at the Meiyu-Baiu-Front in the West Pacific prior to the predictability barrier on 22 June and its interaction with the upper-level jet are important for the preconditioning of the Rossby wave pattern and set the stage for synoptic processes downstream. The predictability barrier of the heat wave at 7 days lead time is thus linked to the misrepresentation of West Pacific synoptic conditions. Nevertheless, the chain of synoptic events after 22 June across the Pacific plays an essential role and additionally limits the predictability of the magnitude of the heat wave. The representation of the heat wave in the ensemble forecasts is thus influenced by a preconditioning of Rossby waves in the West Pacific and limited by synoptic-scale predictability directly prior to the heat wave.

4. Concluding Discussion

In conclusion, our detailed dynamical investigation of the predictability of the Western North American heat wave in June 2021 reveals the dominant role of the downstream development of Rossby waves along the North Pacific jet stream. Diabatic amplification of upper-level Rossby waves due to the outflow of WCB airstreams was essential for establishing the stationary large-scale ridge over Western North America and the development of the unprecedented heat wave which corroborates results of recent studies (Neal et al., 2022). The chain of synoptic events emerged from unusual precipitation along the Meiyu-Baiu-Front >7,000 km upstream over the West Pacific and >10 days prior to the event. Although the seed of the blocking event may be traced back to the Western Pacific or even to Southeast Asia (Lin et al., 2022; Qian et al., 2022), a successful prediction of the heat wave hinges on the successful prediction of the Eastern Pacific synoptic events, and the forecasts initialized before June 22 are not well-conditioned to predict this event accurately. Thus, the complicated scale-interactions involved in the WCB activity, jet amplification, and downstream development constitute a predictability barrier that make accurate forecasts of the heat wave magnitude very unlikely beyond 7 days lead time. The short lead time due to insufficient medium-range forecasts in this case may have hampered possible disaster mitigation efforts. On the first sight, our findings contrast the fact that the predictability horizon of extremely hot temperatures exceeds the predictability horizon of just above-normal temperature anomalies (Wulff & Domeisen, 2019). However, we focus on the prediction of the exact heat wave magnitude and find that it can only be predicted at lead times of <1 week in this case. Notwithstanding, the likelihood of above-normal temperatures and therefore predictability of the potential for a hot extreme was increased, even at subseasonal lead times (Emerton et al., 2022).

The presence of a predictability barrier due to diabatic processes, in particular WCBs and synoptic activity, was also found for other regions, seasons, and extremes (González-Alemán et al., 2022; Sánchez et al., 2020) and deserves further investigation. The emerging picture that atmospheric dynamical processes on the relatively short synoptic time scales matter for high-amplitude Rossby waves and states of the jet stream also has implications

for understanding the consequences of climate change. It is postulated that stationary high-amplitude Rossby waves become more frequent under climate change (Coumou et al., 2018; Hoskins & Woollings, 2015). In a warmer climate, more moisture will be available for latent heat release which may ultimately affect the amplitude of Rossby waves in the way described here. This is also implied by Steinfeld et al. (2022) who showed that the increasing strength and size of atmospheric blocking in a strongly warming climate scale linearly with increased diabatic heating contributions from WCBs. To date, the impact of WCB activity in a future climate is uncertain, in part because of the tug-of-war between potentially increased diabatic heating and concomitant higher isentropic outflow levels of diabatically enhanced weather systems (Joos et al., 2023), and a predicted weakening of dry dynamics/dry synoptic activity (Coumou et al., 2018) through Arctic amplification (Cohen et al., 2014) and the concomitant weakening of midlatitude baroclinicity. Yet, more work is needed to better understand if WCB activity and synoptic dynamics are accurately represented in climate models and lead to more amplified states of the jet stream in the future.

Data Availability Statement

ERA5 data are freely available at <https://doi.org/10.24381/cds.bd0915c6>. ECMWF ensemble forecast data are available through the TIGGE archive from <https://apps.ecmwf.int/datasets/data/tigge/levtype=sfc/type=cf>. The relaxation experiments are accessible through the public KITOpenData repository (<https://doi.org/10.5445/IR/1000152175>). The relevant data from the relaxation experiments are shown in Figures S5 and S6 in Supporting Information S1. GPM IMERG precipitation data are freely available from <https://doi.org/10.5067/GPM/IMERGDF/DAY/06>. The LAGRANTO documentation and information on how to access the source code are provided in Sprenger and Wernli (2015). Information and the source code for the convolutional neural networks model ELIAS 2.0 are available from Quinting and Grams (2022a, 2022b) and Quinting et al. (2022).

References

- Abraham, J. (2021). Record-breaking heat in Canada. Retrieved from <https://www.rmets.org/metmatters/record-breaking-heat-canada>
- Ahmadi-Givi, F., Graig, G. C., & Plant, R. S. (2004). The dynamics of a midlatitude cyclone with very strong latent-heat release. *Quarterly Journal of the Royal Meteorological Society*, 130, 295–323. <https://doi.org/10.1256/qj.02.226>
- Bieli, M., Pfahl, S., & Wernli, H. (2015). A Lagrangian investigation of hot and cold temperature extremes in Europe. *Quarterly Journal of the Royal Meteorological Society*, 141, 98–108. <https://doi.org/10.1002/qj.2339>
- Capucini, M., & Samenow, J. (2021). Heat wave blasts U.S. with 150 million Americans under alerts. Retrieved from <https://www.washingtonpost.com/weather/2021/08/11/heatwave-united-states-pacific-northwest/>
- Cohen, J., Screen, J. A., Furtado, J. C., Barlow, M., Whittleston, D., Coumou, D., et al. (2014). Recent Arctic amplification and extreme mid-latitude weather. *Nature Geoscience*, 7(9), 627–637. <https://doi.org/10.1038/ngeo2234>
- Coumou, D., Di Capua, G., Vavrus, S., Wang, L., & Wang, S. (2018). The influence of Arctic amplification on mid-latitude summer circulation. *Nature Communications*, 9(1), 2959. <https://doi.org/10.1038/s41467-018-05256-8>
- Ding, Y., & Chan, J. C. (2005). The East Asian summer monsoon: An overview. *Meteorology and Atmospheric Physics*, 89(1–4), 117–142. <https://doi.org/10.1007/s00703-005-0125-z>
- Emerton, R., Brimicombe, C., Magnusson, L., Roberts, C., Di Napoli, C., Cloke, H. L., & Pappenberger, F. (2022). Predicting the unprecedented: Forecasting the June 2021 Pacific Northwest heatwave. *Weather*, 77(8), 272–279. <https://doi.org/10.1002/wea.4257>
- Fischer, E. M., Sippel, S., & Knutti, R. (2021). Increasing probability of record-shattering climate extremes. *Nature Climate Change*, 11(8), 689–695. <https://doi.org/10.1038/s41558-021-01092-9>
- González-Alemán, J. J., Grams, C. M., Ayarzagüena, B., Zurita-Gotor, P., Domeisen, D. I., Gómara, I., et al. (2022). Tropospheric role in the predictability of the surface impact of the 2018 sudden stratospheric warming event. *Geophysical Research Letters*, 49, e2021GL095464. <https://doi.org/10.1029/2021GL095464>
- Grams, C. M., & Archambault, H. M. (2016). The key role of diabatic outflow in amplifying the midlatitude flow: A representative case study of weather systems surrounding Western North Pacific extratropical transition. *Monthly Weather Review*, 144(10), 3847–3869. <https://doi.org/10.1175/MWR-D-15-0419.1>
- Grams, C. M., Jones, S. C., Davis, C. A., Harr, P. A., & Weissmann, M. (2013). The impact of Typhoon Jangmi (2008) on the midlatitude flow. Part I: Upper-level ridge building and modification of the jet. *Quarterly Journal of the Royal Meteorological Society*, 139, 2148–2164. <https://doi.org/10.1002/qj.2091>
- Grams, C. M., Magnusson, L., & Madonna, E. (2018). An atmospheric dynamics perspective on the amplification and propagation of forecast error in numerical weather prediction models: A case study. *Quarterly Journal of the Royal Meteorological Society*, 144, 2577–2591. <https://doi.org/10.1002/qj.3353>
- Hauser, S., Teubler, F., Riemer, M., Knippertz, P., & Grams, C. M. (2022). Towards a diagnostic framework unifying different perspectives on blocking dynamics: Insight into a major blocking in the North Atlantic-European region. *Weather and Climate Dynamics Discussions*. <https://doi.org/10.5194/wcd-2022-44>
- Haynes, P. H., & McIntyre, M. E. (1987). On the evolution of vorticity and potential vorticity in the presence of diabatic heating and frictional or other forces. *Journal of the Atmospheric Sciences*, 44(5), 828–841. [https://doi.org/10.1175/1520-0469\(1987\)044<0828:OTEOVA>2.0.CO;2](https://doi.org/10.1175/1520-0469(1987)044<0828:OTEOVA>2.0.CO;2)
- Hersbach, H., Bell, B., Berrisford, P., Hirahara, S., Horányi, A., Muñoz-Sabater, J., et al. (2020). The ERA5 global reanalysis. *Quarterly Journal of the Royal Meteorological Society*, 146, 1999–2049. <https://doi.org/10.1002/qj.3803>

Acknowledgments

This work was funded by the Helmholtz Association as part of the Young Investigator Group “Subseasonal Predictability: Understanding the Role of Diabatic Outflow” (SPREADOUT, Grant VH-NG-1243). The research was partially embedded in the subprojects A8 and B8 of the Transregional Collaborative Research Center SFB/TRR 165 “Waves to Weather” (<https://www.wavestoweather.de>, last access: 01/2022) funded by the German Research Foundation (DFG). The authors acknowledge support by the state of Baden-Württemberg through bwHPC. ECMWF is acknowledged for granting access to the reanalysis data sets and operational ensemble forecast data. We thank the anonymous reviewer and Dr. Ruping Mo for their positive and constructive feedback that helped to improve the quality of the manuscript.

- Hoskins, B. J., McIntyre, M. E., & Robertson, A. W. (1985). On the use and significance of isentropic potential vorticity maps. *Quarterly Journal of the Royal Meteorological Society*, *111*, 877–946. <https://doi.org/10.1002/qj.49711147002>
- Hoskins, B. J., & Woollings, T. (2015). Persistent extratropical regimes and climate extremes. *Current Climate Change Reports*, *1*(3), 115–124. <https://doi.org/10.1007/s40641-015-0020-8>
- Huffman, G., Stocker, E., Bolvin, D., Nelkin, E., & Tan, J. (2019). *GPM IMERG final precipitation L3 1 day 0.1 degree × 0.1 degree V06*. In A. Savičenko, & M. D. Greenbelt (Eds.), *Goddard Earth Sciences Data and Information Services Center (GES DISC)* [Dataset]. <https://doi.org/10.5067/GPM/IMERGDF/DAY/06>
- Joos, H., Sprenger, M., Binder, H., Beyerle, U., & Wernli, H. (2023). Warm conveyor belts in present-day and future climate simulations – Part I: Climatology and impacts. *Weather and Climate Dynamics*, *4*(1), 133–155. <https://doi.org/10.5194/wcd-4-133-2023>
- Kornhuber, K., Coumou, D., Vogel, E., Lesk, C., Donges, J. F., Lehmann, J., & Horton, R. M. (2020). Amplified Rossby waves enhance risk of concurrent heatwaves in major breadbasket regions. *Nature Climate Change*, *10*(1), 48–53. <https://doi.org/10.1038/s41558-019-0637-z>
- Lin, H., Mo, R., & Vitart, F. (2022). The 2021 Western North American heatwave and its subseasonal predictions. *Geophysical Research Letters*, *49*, e2021GL097036. <https://doi.org/10.1029/2021GL097036>
- Madonna, E., Wernli, H., Joos, H., & Martius, O. (2014). Warm conveyor belts in the ERA-Interim Dataset (1979–2010). Part I: Climatology and potential vorticity evolution. *Journal of Climate*, *27*(1), 3–26. <https://doi.org/10.1175/JCLI-D-12-00720.1>
- Magnusson, L. (2017). Diagnostic methods for understanding the origin of forecast errors. *Quarterly Journal of the Royal Meteorological Society*, *143*, 2129–2142. <https://doi.org/10.1002/qj.3072>
- Mo, R., Lin, H., & Vitart, F. (2022). An anomalous warm-season trans-Pacific atmospheric river linked to the 2021 Western North America heatwave. *Communications Earth & Environment*, *3*(1), 127. <https://doi.org/10.1038/s43247-022-00459-w>
- Neal, E., Huang, C. S., & Nakamura, N. (2022). The 2021 Pacific northwest heat wave and associated blocking: Meteorology and the role of an upstream cyclone as a diabatic source of wave activity. *Geophysical Research Letters*, *49*, e2021GL097699. <https://doi.org/10.1029/2021GL097699>
- Ninomiya, K., & Shibagaki, Y. (2007). Multi-scale features of the Meiyu-Baiu front and associated precipitation systems. *Journal of the Meteorological Society of Japan*, *85B*, 103–122. <https://doi.org/10.2151/jmsj.85B.103>
- Petoukhov, V., Petri, S., Rahmstorf, S., Coumou, D., Kornhuber, K., & Schellnhuber, H. J. (2016). Role of quasiresonant planetary wave dynamics in recent boreal spring-to-autumn extreme events. *Proceedings of the National Academy of Sciences of the United States of America*, *113*(25), 6862–6867. <https://doi.org/10.1073/pnas.1606300113>
- Pfahl, S., Schwierz, C., Croci-Maspoli, M., Grams, C. M., & Wernli, H. (2015). Importance of latent heat release in ascending air streams for atmospheric blocking. *Nature Geoscience*, *8*(8), 610–614. <https://doi.org/10.1038/ngeo2487>
- Pfahl, S., & Wernli, H. (2012). Quantifying the relevance of atmospheric blocking for co-located temperature extremes in the Northern Hemisphere on (sub-)daily time scales. *Geophysical Research Letters*, *39*, L12807. <https://doi.org/10.1029/2012GL052261>
- Philip, S. Y., Kew, S. F., Oldenborgh, G. J. V., Yang, W., Vecchi, G. A., Anslow, F. S., et al. (2021). Rapid attribution analysis of the extraordinary heatwave on the Pacific Coast of the US and Canada June 2021 (pp. 119–123). *World Weather Attribution*. <https://doi.org/10.5194/esd-2021-90>
- Qian, Y., Hsu, P. C., Yuan, J., Zhu, Z., Wang, H., & Duan, M. (2022). Effects of subseasonal variation in the East Asian monsoon system on the summertime heat wave in Western North America in 2021. *Geophysical Research Letters*, *49*, e2021GL097659. <https://doi.org/10.1029/2021GL097659>
- Quinting, J. F., & Grams, C. M. (2021). EuLerian Identification of ascending AirStreams (ELIAS 2.0) in numerical weather prediction and climate models—Part 1: Development of deep learning model [code]. *Zenodo*. <https://doi.org/10.5281/zenodo.5154980>
- Quinting, J. F., & Grams, C. M. (2022). EuLerian Identification of ascending AirStreams (ELIAS 2.0) in numerical weather prediction and climate models—Part 1: Development of deep learning model. *Geoscientific Model Development*, *15*(2), 715–730. <https://doi.org/10.5194/gmd-15-715-2022>
- Quinting, J. F., Grams, C. M., Oertel, A., & Pickl, M. (2022). EuLerian Identification of ascending AirStreams (ELIAS 2.0) in numerical weather prediction and climate models—Part 2: Model application to different datasets. *Geoscientific Model Development*, *15*(2), 731–744. <https://doi.org/10.5194/gmd-15-731-2022>
- Quinting, J. F., & Reeder, M. J. (2017). Southeastern Australian heat waves from a trajectory viewpoint. *Monthly Weather Review*, *145*(10), 4109–4125. <https://doi.org/10.1175/MWR-D-17-0165.1>
- Sánchez, C., Methven, J., Gray, S., & Cullen, M. (2020). Linking rapid forecast error growth to diabatic processes. *Quarterly Journal of the Royal Meteorological Society*, *146*, 3548–3569. <https://doi.org/10.1002/qj.3861>
- Screen, J. A., & Simmonds, I. (2014). Amplified mid-latitude planetary waves favour particular regional weather extremes. *Nature Climate Change*, *4*(8), 704–709. <https://doi.org/10.1038/nclimate2271>
- Seneviratne, S. I., Zhang, X., Adnan, M., Badi, W., Dereczynski, C., Di Luca, A., et al. (2021). Weather and climate extreme events in a changing climate [Book Section]. In V. Masson-Delmotte, P. Zhai, A. Pirani, S. L. Connors, C. Pean, Y. Chen, et al. (Eds.), *Climate change 2021: The physical science basis. contribution of working group I to the sixth assessment report of the intergovernmental panel on climate change* (pp. 1513–1766). Cambridge University Press. <https://doi.org/10.1017/9781009157896.013>
- Spensberger, C., Madonna, E., Boettcher, M., Grams, C. M., Papritz, L., Quinting, J. F., et al. (2020). Dynamics of concurrent and sequential Central European and Scandinavian heatwaves. *Quarterly Journal of the Royal Meteorological Society*, *146*, 2998–3013. <https://doi.org/10.1002/qj.3822>
- Sprenger, M., & Wernli, H. (2015). The LAGRANTO Lagrangian analysis tool—Version 2.0. *Geoscientific Model Development*, *8*(8), 2569–2586. <https://doi.org/10.5194/gmd-8-2569-2015>
- Steinfeld, D., & Pfahl, S. (2019). The role of latent heating in atmospheric blocking dynamics: A global climatology. *Climate Dynamics*, *53*(9–10), 6159–6180. <https://doi.org/10.1007/s00382-019-04919-6>
- Steinfeld, D., Sprenger, M., Beyerle, U., & Pfahl, S. (2022). Response of moist and dry processes in atmospheric blocking to climate change. *Environmental Research Letters*, *17*(8), 084020. <https://doi.org/10.1088/1748-9326/ac81af>
- Teng, H., Branstator, G., Wang, H., Meehl, G. A., & Washington, W. M. (2013). Probability of US heat waves affected by a subseasonal planetary wave pattern. *Nature Geoscience*, *6*(12), 1056–1061. <https://doi.org/10.1038/ngeo1988>
- Wernli, H., & Davies, H. C. (1997). A Lagrangian-based analysis of extratropical cyclones. I: The method and some applications. *Quarterly Journal of the Royal Meteorological Society*, *123*, 467–489. <https://doi.org/10.1002/qj.49712353811>

- White, C. J., Carlsen, H., Robertson, A. W., Klein, R. J., Lazo, J. K., Kumar, A., et al. (2017). Potential applications of subseasonal-to-seasonal (S2S) predictions. *Meteorological Applications*, *24*(3), 315–325. <https://doi.org/10.1002/met.1654>
- Wulff, C. O., & Domeisen, D. I. (2019). Higher subseasonal predictability of extreme hot European summer temperatures as compared to average summers. *Geophysical Research Letters*, *46*, 11520–11529. <https://doi.org/10.1029/2019GL084314>
- Zschenderlein, P., Fink, A. H., Pfahl, S., & Wernli, H. (2019). Processes determining heat waves across different European climates. *Quarterly Journal of the Royal Meteorological Society*, *145*, 2973–2989. <https://doi.org/10.1002/qj.3599>